Chinese Chemical Letters 37 (2026) 111593

Contents lists available at ScienceDirect

Chinese Chemical Letters

journal homepage: www.elsevier.com/locate/cclet

Underscoring the polyimide-linkage in covalent organic frameworks and related applications

Qi Li[a,1], Minqiao Liang[a,1], Huifen Zhuang[a], Zhengyang Chen[a], Yuxiang Jiang[a], Xiaofei Chen[b,*], Yifa Chen[a,*], Ya-Qian Lan[a,*]

[a] School of Chemistry, South China Normal University, Guangzhou 510006, China
[b] Key Laboratory for Special Functional Materials of Ministry of Education National & Local Joint Engineering Research Center for High-Efficiency Display and Lighting Technology, School of Nanoscience and Materials Engineering, Henan University, Kaifeng 475004, China

ARTICLE INFO

Article history:
Received 11 May 2025
Revised 8 July 2025
Accepted 16 July 2025
Available online 18 July 2025

Keywords:
Covalent organic frameworks
Polyimide-linkage
Heteroatomic sites
Chemical stability
Thermal stability

ABSTRACT

Polyimide-linkage covalent organic frameworks (PI-COFs), as a subclass of the COFs material family, featuring the unique combination of excellent thermal stability of polyimide, tunable pore sizes, as well as high crystallinity and surface area of COFs, are expected to be a novel type of promising crystalline porous material with potential applications in adsorption and separation, catalysis, chemical sensing, and energy storage. Therefore, it is increasingly important to summarize polyimide-linkage in COFs and related applications and provide in-depth insight to accelerate future development. In this review, we offer a comprehensive overview of recent advancements in PI-COFs, emphasizing their synthesis methods, design principles and applications. Finally, our brief outlooks on the current challenges and future developments of PI-COFs are provided. Overall, this review aims to guide the recent and future development of PI-COFs.

© 2025 Published by Elsevier B.V. on behalf of Chinese Chemical Society and Institute of Materia Medica, Chinese Academy of Medical Sciences.

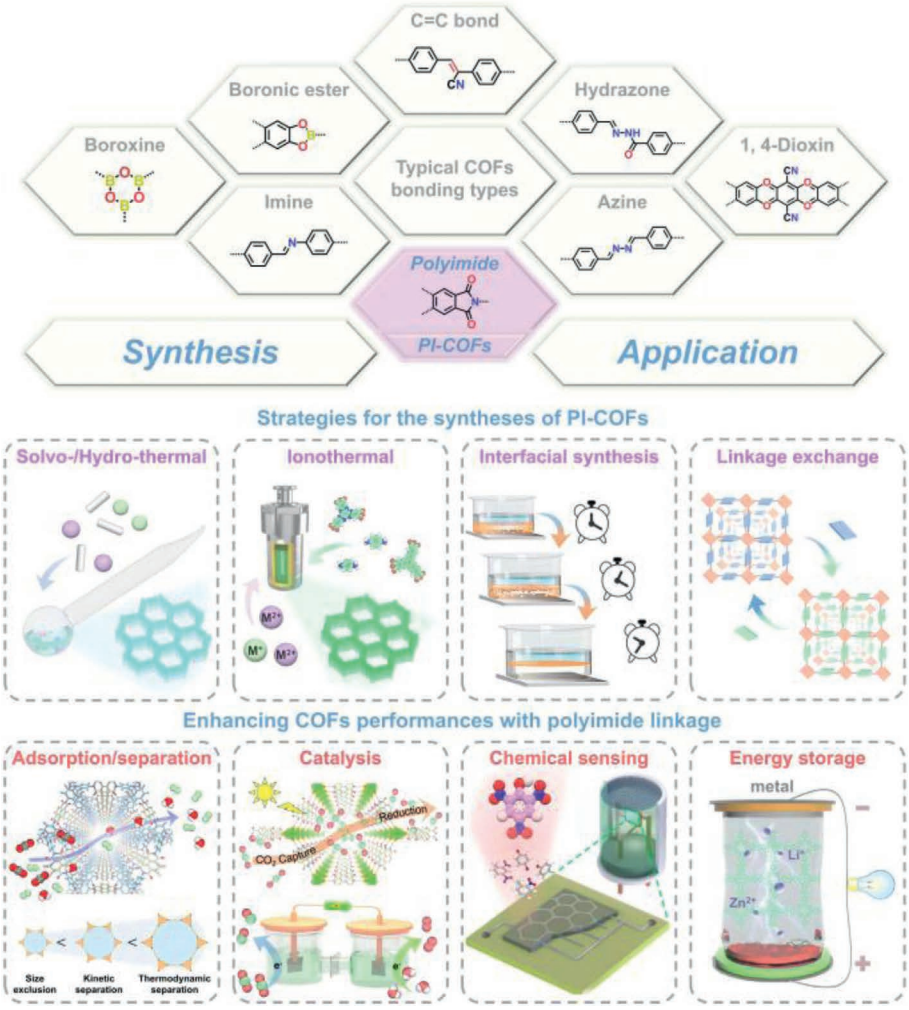
1. Introduction

Polyimide (PI) polymers refer to a class of high-temperature polymers with imide rings (−CO−NR−CO−) in the main chain [1]. Although the synthesis of PI was first reported in 1908, it was not until the early 1960s that a successful commercial route to high-molecular-weight PI was first patented by DuPont. PI polymers are formed through a polycondensation reaction between dianhydride and aromatic amine monomers, consisting of electron-donating (amine) and electron-accepting (anhydride) groups within a single conjugated skeleton, which enables both intermolecular and intramolecular charge transfer [2]. Thanks to the uniqueness of the PI structure, compared with other polymer materials, the presence of multiple imide bonds enables the PI polymers to withstand high-temperature environments (exceeding 400 °C) and offer exceptional mechanical strength (seven times stronger than steel) along with chemical stability and reversible electron transfer property, making them applicable in the aerospace, separating membranes, microelectronics, or semiconductor fields [3–7]. In the latest 2000s, amorphous but intrinsically microporous aromatic PIs were prepared with spirobifluorene units as a structure-directing motif [8–10]. Even though microporous PI polymers show good thermal stability, their applications are still limited, primarily due to their low specific surface area, non-uniform pore size and unclear structures. If the crystallinity and porosity could be combined into PI polymers to extend the field of crystalline materials, more advanced functions might be introduced. Therefore, crystalline and porous PIs urgently need to be explored to bring new insights into this field.

Polyimide-linkage covalent organic frameworks (PI-COFs), a class of crystalline porous materials first reported by Yan *et al.* in 2014, integrate the structural tunability and crystallinity of COFs with the robustness of PI linkages (Scheme 1 and Fig. 1) [11]. They inherit excellent thermal and chemical stability from PIs while maintaining the porosity and crystallinity of traditional COFs [12–20]. By integrating the PI backbone into the COFs structures, PI-COFs achieve broader functionality and enhanced adjustability [21–30]. These features make PI-COFs promising for diverse applications including adsorption/separation, photo-/electro-electrocatalysis, energy storage, and sensing. In particular, PI-COFs offer several unique advantages: (1) Electronegative heteroatoms (*e.g.*, N, O) enable strong metal coordination and electron-density modulation [31]; (2) bipolar active centers (C=O and C−N) support

* Corresponding authors.
E-mail addresses: chenxf22@henu.edu.cn (X. Chen), chenyf927821@163.com (Y. Chen), yqlan@m.scnu.edu.cn (Y.-Q. Lan).
[1] These authors contributed equally to this work.

https://doi.org/10.1016/j.cclet.2025.111593
1001-8417/© 2025 Published by Elsevier B.V. on behalf of Chinese Chemical Society and Institute of Materia Medica, Chinese Academy of Medical Sciences.



Scheme 1. Schematic illustration of the synthesis strategies and applications of PI-COFs.

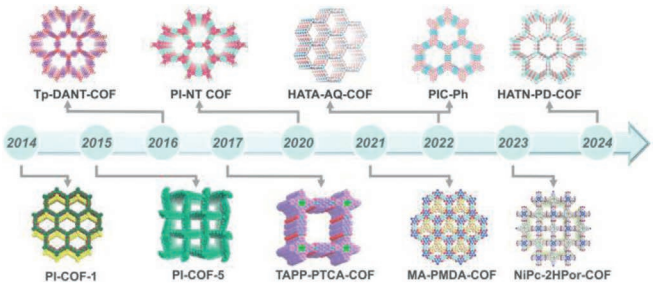


Fig. 1. The development timeline of representative PI-COFs. Image for PI-COF-1: Reproduced with permission [11]. Copyright 2014, Springer Nature. Image for PI-COF-5: Reproduced with permission [12]. Copyright 2015, American Chemical Society. Image for Tp-DANT-COF: Reproduced with permission [13]. Copyright 2016, Royal Society of Chemistry. Image for TAAP-PTCA-COF: Reproduced with permission [14]. Copyright 2017, American Chemical Society. Image for PI-NT COF: Reproduced with permission [15]. Copyright 2020, American Chemical Society. Image for MA-PMDA-COF: Reproduced with permission [16]. Copyright 2021, American Chemical Society. Image for HATA-AQ-COF and PIC-pH: Reproduced with permission [17,18]. Copyright 2022, Wiley-VCH. Image for NiPc-2HPor COF: Reproduced with permission [19]. Copyright 2023, Oxford University Press. Image for HATN-PD-COF: Reproduced with permission [20]. Copyright 2024, Springer Nature.

fast ion transport and storage [32]; (3) carbonyl-rich PI units could introduce redox-active sites [33]; (4) the robust PI linkage ensures stability under harsh conditions [34]; and (5) reactive aromatic units allow versatile structural tuning and modification [35]. Together, these attributes define the distinct position of PI-COFs among COF materials and underscore their potential for functional applications.

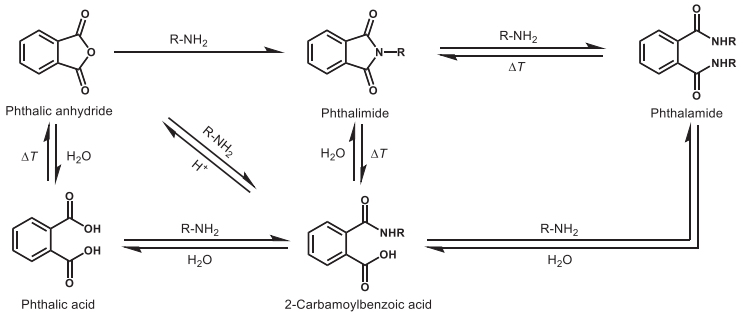
Toward the future development of PI-COFs, this review presents a comprehensive overview of recent advances in PI-COFs including design principles, synthesis strategies and their applications in adsorption/separation, catalysis, chemical sensing, and energy storage, *etc.* (Scheme 1). Furthermore, we intend to establish the associations between the functions of PI-COFs and their applications, and evaluate their performances from structural design to mechanism exploration. Finally, our perspectives on current challenges and future prospects of PI-COFs are briefly discussed. We aim this review to provide more readers with a comprehensive understanding of PI-COFs, encompassing fundamental concepts, synthesis strategies, and functionalities as well as elucidating the structure-to-property relationships to facilitate their development and applications.

2. Design and preparation methods

2.1. Design principles of PI-COFs

The strategy for preparing PI-linkage COFs involves the imidization of extended acetic anhydride/dicarboxylic acid and amine derivatives building units [36]. As we know, the imide linkage reaction usually has poor reversibility of polyimidization and requires

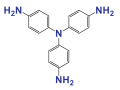
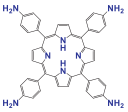
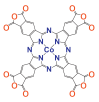
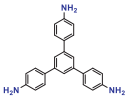
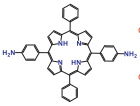
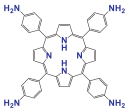
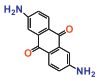
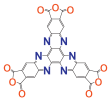
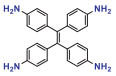
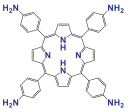
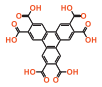
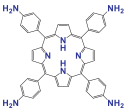
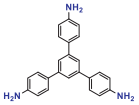
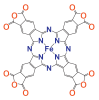
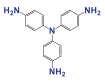
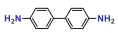
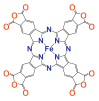
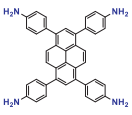
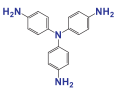
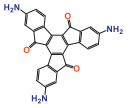
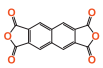
Table 1
Possible reaction mechanism (taking phthalic anhydride as the model substrate) and reported representative PI-COFs.



PI-COFs	Ligand 1	Ligand 2	Pore size (nm)	S_{BET} (m^2/g) [c]	Appl. [a] and Ref.	PI-COFs	Ligand 1	Ligand 2	Pore size (nm)	S_{BET} (m^2/g)[c]	Appl. [a] and Ref.
$COF_{TPDA-PMDA}$	TPDA	PMDA	2.7	2669	LIBs [40]	TAPB-PTCDA-COF	TAPB	PTCDA	3.1	460	– [b] [39]
PI-COF-4	TAA	PMDA	1.3	2403	Drug delivery [12]	CoPcPI-COF-3	TAPA	CoPc	1.2	415	Electrocatalysis [51]
PI-COF-3	TABPB	PMDA	5.3	2346	Adsorption [11]	ZnPc-DPA-COF	PDA	ZnPc	2.0	287	Infrared photocatalysis [43]
PI-COF-5	TAPM	PMDA	1.0	1876	Drug delivery [12]	NiPcc-2HPor-COF	TAPP	NiPcc	1.45	258	Electrocatalysis [19]
PI-COF-2	TAPB	PMDA	3.7	1297	Adsorption [11]	COF-JLU85	TRO	PMDA	3.3	215	LIBs [42]
TAPB-PMDA-COF	TAPB	PMDA	2.9	1250	– [39]	PI-COF	MA	PMDA	1.3	146	LSBs [16]
HATN-PD-COF	PD	HATNCA	3.1	1200	SIBs [20]	PIC-Dp	BD	TPHCA	–	125	LIBs [18]
TTTA-PMDA-COF	TT	PMDA	3.0	1083	RABs [33]	PIC-Tp	TD	TPHCA	–	54	LIBs [18]
HATN-TAB-COF	TAPB	HATNCA	2.0	1065	SIBs [20]	NiPc-OH-COF	R=OH,CH_3,H	NiPc	1.94	53	Electrocatalysis [44]

(*continued on next page*)

Table 1 (*continued*)

PI-COFs	Ligand 1	Ligand 2	Pore size (nm)	S_{BET} (m^2/g) [c]	Appl. [a] and Ref.	PI-COFs	Ligand 1	Ligand 2	Pore size (nm)	S_{BET} (m^2/g)[c]	Appl. [a] and Ref.
PI-COF-1	 TAPA	 PMDA	3.3	1027	Adsorption [11]	CoPc-2H_2Por	 TAPP	 CoPc	3.72	38.6	Electrocatalysis [45]
PIC (NTCDA-TAPB)	 TAPB	 PTCDA	3.10	990	SIBs [34]	CoPc-2H_2Por	 DAPP	 CoPc	2.12	27.7	Electrocatalysis [45]
PI-COFs	 TAPP	 PTCDA	2.7	894	Sensing [14]	PI-COF 202	 MA	 PTCDA	1.68	9.161	Sensing [46]
HATN-AQ-COF	 DAAQ	 HATN-AP	3.8	725	LIBs [17]	PI-COF 201	 MA	 PMDA	1.72	3.929	Sensing [46]
TAPE-PMDA-COF	 TAPE	 PMDA	2.6	689	– [41]	2DPI	 TAPP	 PTCDA	3.0	–	– [47]
PIC-Ph	 PD	 TPHCA	–	669	LIBs [18]	2DPA	 TAPP	 PMDA	2.02	–	– [47]
PIA	 TAPB	 PMDA	3.19	580	CO_2 adsorption [34]	FePc-PI-COF-1	PD	 FePc	2.0	–	Electrocatalysis [49]
PI-NT-COF	 TAPA	 NTCDA	3.3	576	Resistive memory devices [15]	FePc-PI-COF-2	 BD	 FePc	2.3	–	Electrocatalysis [49]
PICOF-1	 PyTTTA	 PMDA	1.03	510	– [41]	PI-COF	 TAPA	 PTCDA	2.5-3.2		ZIBs [50]
COF-JLU86	 TRO	 NTCDA	3.5	491	LIBs [42]						

[a] "Appl." refers to the abbreviation of "Application".
[b] "–" represents not mentioned in the text.
[c] Sorted by BET surface area

a temperature of about 250 °C [11]. However, depending on the reaction conditions, the formation of imide bonds can be reversible [37]. Taking the phthalic anhydride as the model substrate (Table 1), it reacts with an aniline molecule, and an H_2O molecule is eliminated to yield an imide intermediate, phthalimide. The formed phthalimide can react with an excess of amine to produce phthalimide, which can be converted back under high-temperature conditions. Even if 2-carbanoylbenzoic acid is further generated at high temperatures, phthalimide can also be reformed through a hydration reaction. 2-Carbanoylbenzoic acid can be transformed into ph-

thalic anhydride or phthalic acid by reaction with H_2O and H^+, and it can also be reacted reversibly with an amine. If phthalic anhydride could be hydrolyzed to form phthalic acid, the reaction can be back under high temperature (about 250 °C). In summary, a dynamic equilibrium is established among phthalic anhydride, intermediates and phthalimide at high temperatures in the presence of base. Elevated temperature and the absence of H_2O would favor the formation of phthalimide over other reaction products. Therefore, the reversibility of PI bonds is more conducive to the preparation of highly crystalline PI-COFs. Based on these, plentiful organic ligands have been selected for the building blocks of PI-COFs and recently reported PI-COFs as well as the pore size, Brunauer-Emmett-Teller surface area (S_{BET}), and their functions, have been outlined in Table 1.

As we know, the directional construction of various COFs can be guided by pre-designed topologies, which rely on the connectivity and geometry of discrete organic building blocks [38,39]. In essence, PI-COFs are usually synthesized with two monomers, bis, tri or tetra-aromatic primary amine and aromatic conjugated anhydride, in which the amine and anhydride act as node and linker, respectively. In general, the aromatic primary amines, usually have many options, *e.g.*, *C_2-symmetry*, *C_3-symmetry* and *C_4-symmetry* molecules. The available aromatic anhydrides are mainly two-fold symmetric monomers, limited to the low-yield synthesis of three, four-fold symmetrical molecules, only several types of molecules have been reported. Given the building blocks have definite topological structures and rigid structures, topology such as hexagonal ("C_3+C_2"), square or quasi-square ("C_4+C_2", "C_4+C_4"), rectangular and star-shape in 2D PI-COFs have been formed [38,40–50]. With the rapid development of synthetic technology, quite recently, few 3D PI-COFs ("$T_d + C_2$", "$T_d + C_4$") and interpenetration structures have also been constructed [12,51]. More recently, the sophisticated molecular design of COFs has gradually shifted the focus from structural diversity to the practical applicability of their functions. Therefore, PI-COFs can be constructed into diverse structures by tailoring the corresponding organic nodes and linker configurations.

2.2. The preparation methods of PI-COFs

The formation of reversible covalent bonds allows for self-healing and self-error correction during the crystallization process, which helps to prevent the formation of disordered amorphous kinetic products, resulting in crystalline thermodynamic products [52]. Moreover, relevant factors of monomers such as solubility, and reaction conditions (*e.g.*, temperature, pressure, pH or time) and other influencing factors should be considered [53]. To date, PI-COFs have been synthesized using various methods [54]. In this part, the advantages and disadvantages of many typical PI-COFs preparation methods (*e.g.*, solvothermal synthesis, ionothermal synthesis, hydrothermal synthesis, interfacial synthesis and linkage exchange strategy) are discussed and critically compared regarding their key parameters such as reaction conditions, crystallinity, and porosity (Fig. 2).

2.2.1. Solvothermal synthesis

Solvothermal synthesis is the most classic synthesis method for PI-COFs. This method usually needs to be heated (about 250 °C) for 5–7 days in a sealed Pyrex tube [55]. Commonly, the Pyrex tube is firstly charged with ligands and solvents, frozen with liquid nitrogen, then freeze-vacuum-thaw several times to remove oxygen from the tube; afterward, the Pyrex tube is sealed and heated for a certain time; finally, the obtained PI-COFs are treated with multi-step purification steps to yield final products. The vast majority of

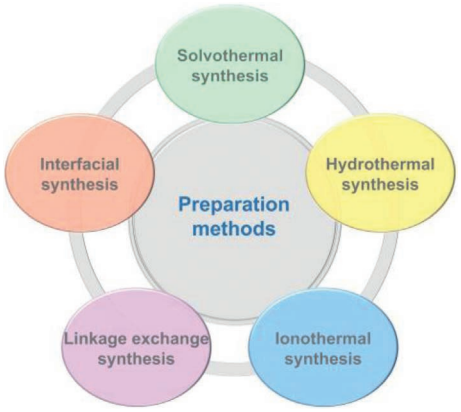


Fig. 2. The main preparation methods of PI-COFs.

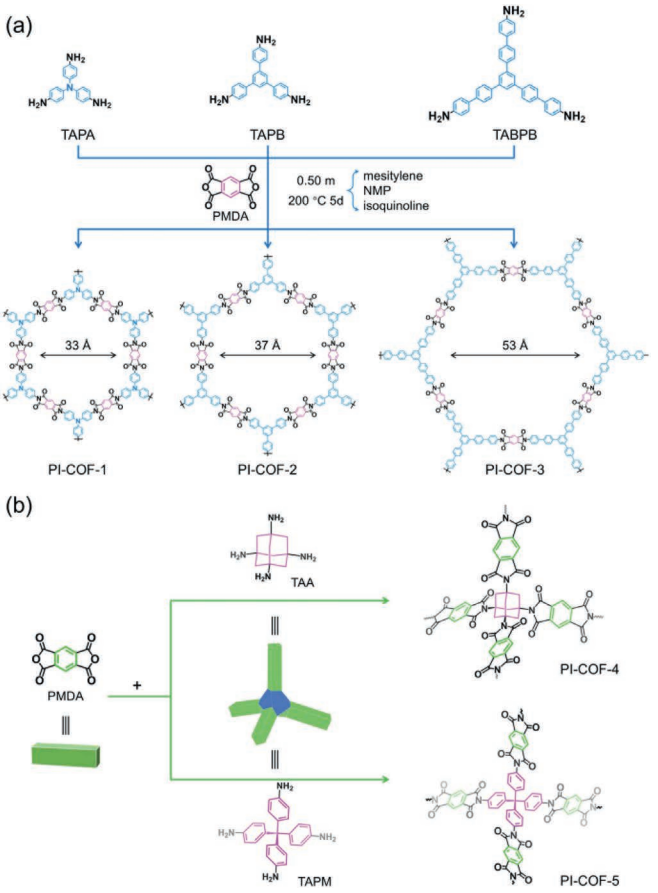


Fig. 3. Strategy for preparing 2D or 3D porous crystalline PI-COFs under solvothermal conditions. (a) 2D PI-COF-1, 2D PI-COF-2 and 2D PI-COF-3. Reproduced with permission [11]. Copyright 2014, Springer Nature. (b) 3D PI-COF-4 and 3D PI-COF-5. Reproduced with permission [12]. Reproduced with permission. Copyright 2015, American Chemical Society.

PI-COFs are synthesized based on this way, as it typically results in favorable crystallinity.

Specifically, in 2014, Yan's group synthesized the first case of PI-COFs (PI-COF-1, PI-COF-2 and PI-COF-3) under solvothermal conditions through the reaction of PMDA and TAPA, TAPB or TABPB under the high-boiling mixed solvents, respectively, followed by heating at 200 or 250 °C for 5 days (Fig. 3a) [11]. These PI-COFs all showed good crystallinity and possessed large pore sizes that could be tuned by extending the length of building units. Particularly, PI-COF-3 displayed a large pore size (5.3 nm). These PI-COFs

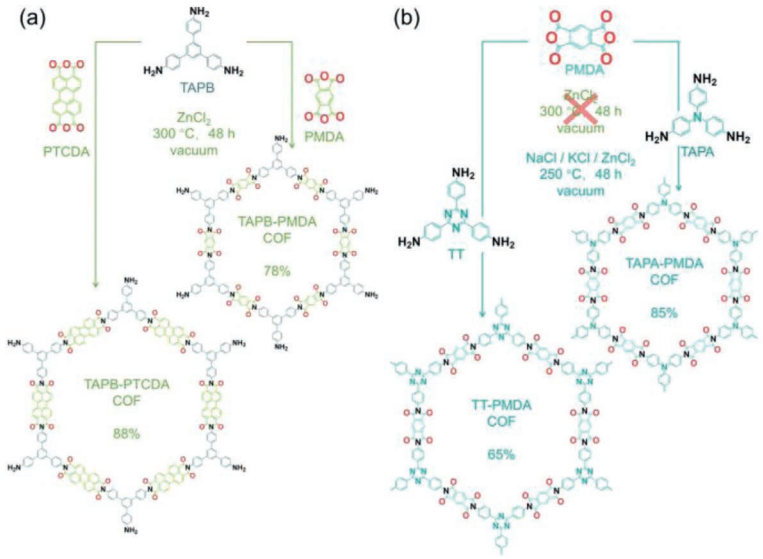


Fig. 4. Schematic illustration for the syntheses of TAPB-based PI-COFs and PMDA-based PI-COFs under ionothermal conditions. (a) In $ZnCl_2$. (b) In an eutectic salt mixture [39].

showed higher surface area (2346 m^2/g) and excellent thermal stability than amorphous PIs. Then, in 2015, using the same linear anhydride building unit (PMDA), they further combined tetrahedral amine monomer TAA and TAPM *via* imidization reaction to design two 3D PI-COFs (PI-COF-4 and PI-COF-5) (Fig. 3b). By choosing tetrahedral building units of different sizes, these PI-COFs featuring non- or interpenetrated structures were obtained and possessed high thermal stability (>450 °C) and high surface area (up to 2403 m^2/g) [12].

Although solvothermal method is widely employed and classic for obtaining high-quality crystalline PI-COFs, it is still confronted with some inevitable drawbacks, such as high-boiling mixed solvents, relatively complicated vacuum and flame treatment procedures. To address these issues, the optimization of solvent systems or reaction temperatures might improve the crystallinity and BET surface areas, while employing additives or templating agents could enhance porosity and pore uniformity. Nevertheless, it is still challenging in preparing PI-COFs in single-crystal forms *via* this method at present. To obtain satisfactory products, specific synthesis conditions and advanced solvothermal techniques might be still needed to facilitate the development of this method.

2.2.2. Ionothermal synthesis

Ionothermal method is another synthesis approach for PI-COFs that utilizes metal salts or eutectic salt mixtures as catalysts and structural directing agents under elevated temperature conditions [56]. Compared to conventional solvothermal methods, this strategy eliminates the need for large quantities of harmful solvents and catalysts, significantly reducing reaction time. It can be conducted at ambient pressure and does not require soluble precursors, while also demonstrating excellent stability.

In 2020, Lotsch's group employed this method to synthesize TAPB-PTCDA-COF and TAPB-PMDA-COF in anhydrous $ZnCl_2$ (Fig. 4a) [39]. The reaction mixture was then heated to 300 °C in a flame-sealed glass tube for 48 h under vacuum, resulting in the generation of crystalline solids. They further demonstrated that for thermally unstable ligands such as TAPA and TT, high crystallinity PI-COF could still be obtained by lowering the reaction temperature and substituting $ZnCl_2$ with an eutectic salt (Fig. 4b). Mechanistic studies indicated that the intermediate formed by the interaction of the two monomers with metal salts may activate the anhydride and imide rings, thereby reducing the overall activation energy and enhancing the reversibility of the PI-COFs formation process. This reversibility is not achievable through traditional methods, yet it is indispensable for the future synthesis of PI-COFs. Very recently, Zhang *et al.* reported an emerging synthesis method for PI-COFs based on organic flux synthesis, which was prepared by using benzoic acid as the flux at 200 or 250 °C for 5 days [57]. Based on this method, a series of low-cost kilogram-scale syntheses of PI-COFs has been achieved, and the world's first ton-scale production line of COFs materials has been built. Considering the influence of heat uniformity, crystallinity and purity in synthesis, there is still much room for further exploration.

2.2.3. Hydrothermal synthesis

Hydrothermal synthesis strategy is an emerging approach for preparing PI-COFs using water as a green solvent, primarily relying on the high-temperature, high-pressure state of water to facilitate chemical reactions between precursors, promote molecular self-assembly and induce crystal growth [58]. Compared to solvothermal methods, hydrothermal synthesis avoids the use of high-boiling, toxic solvents and catalysts.

In 2022, Kim *et al.* developed firstly the geometric hydrothermal synthesis to prepare various highly crystalline PI-COFs with a C_3-*symmetry* hexacarboxylic acid molecule (TPHCA) as the nodes without using catalysts or toxic solvents (Fig. 5a) [18]. They pointed out that the solubility of oligomer intermediates affected the generation of the PI-COFs prepared under hydrothermal conditions. Further mechanisms indicated that the solubility of the oligomeric structure influenced the reaction pathway of the 2D PICs during the development of the 3D stacking structure (*i.e.*, a thermodynamic pathway for PIC-pH and a kinetic pathway for PIC-Dp, Fig. 5b). Afterward, Lostch *et al.* modified this approach for the direct synthesis of PI-COFs *via* alcohol-assisted hydrothermal polyimide (aaHTP) condensation [41]. Very recently, Jiang *et al.* also reported two PI-COFs (*i.e.*, HATN-PD-COF and HATN-TAB-COF) possessing high crystallinity with AA stacking configuration, which were also constructed using the hydrothermal synthesis from the redox-active precursors HATACN and aromatic amines [20].

As a simple, green and low-cost synthesis strategy, hydrothermal synthesis requires further in-depth understanding for its application in the synthesis of PI-COFs. It should be noted that the solubility of the monomers and intermediates in water is crucial for controlling the crystallinity of related PI-COFs. Even though, hy-

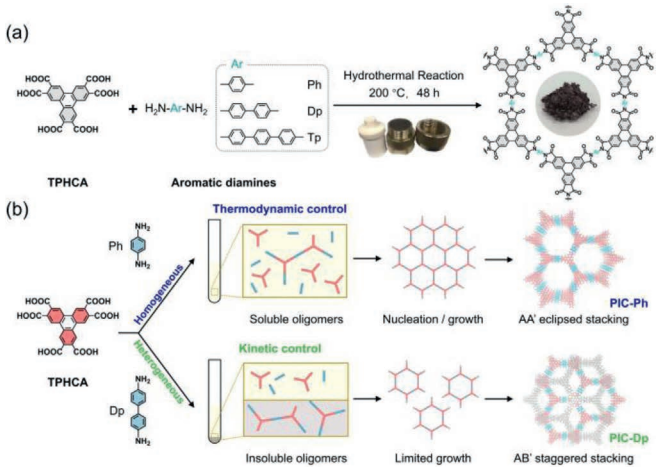


Fig. 5. Synthesis and mechanism of TPHCA-pH/Dp/Tp COFs. (a) Illustration of the hydrothermal synthesis method and (b) the proposed reaction pathways of PIC-pH and PIC-Dp. Reproduced with permission [18]. Copyright 2022, Wiley-VCH.

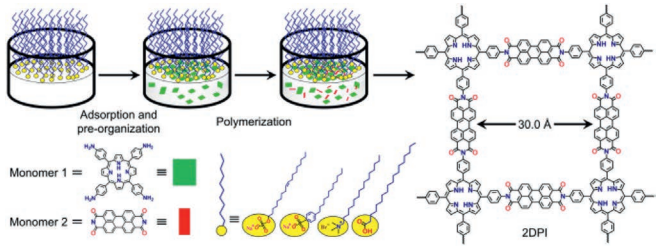


Fig. 6. Synthesis of 2DPI using interfacial synthesis strategy. Reproduced with permission [47]. Copyright 2019, Springer Nature.

drothermal synthesis is still one of the most promising methods to obtain highly crystalline PI-COFs, which can provide accurate structural information, and more efforts are still needed to contribute to this hot topic.

2.2.4. Interfacial synthesis strategy

Interfacial polymerization is a commonly used method for preparing thin-film composite membranes, which can also be applied in the synthesis of PI-COFs. Recently, multilayer PI-COFs films have been successfully synthesized through the reaction at the liquid-liquid or liquid-air interfaces. For example, Feng *et al.* reported the controllable preparation of few-layer 2D PI-COFs on the surface of water through imide reaction, assisted by surfactant monolayers (Fig. 6) [47]. The resulting PI-COFs exhibited high crystallinity, with a thickness of ~2 nm (~5 layers) and an average crystal domain size of ~3.5 μm^2. Theoretical and model experiments demonstrated that self-assembled monolayers can facilitate the preorganization of monomers, accelerating the polymerization kinetics of the monomers at the water surface (gas-liquid interface). This process enables the synthesis of PI-COFs under ambient temperature conditions, which traditionally require high-temperature polymerization.

Apart from this, interfacial synthesis strategy still needs to select a suitable solvent to generate the interfacial layer and dissolve the monomer, which requires high activity at the interfacial layer. Additionally, solvent volatilization and solvent contamination in the preparation process bring about complicated post-treatment problems. Furthermore, local differences in interface control and reaction conditions tend to result in poor homogeneity of materials. As a result, the strong solvent dependence, interface instability, and difficulties in achieving material homogeneity and scalability make the widespread application challenging.

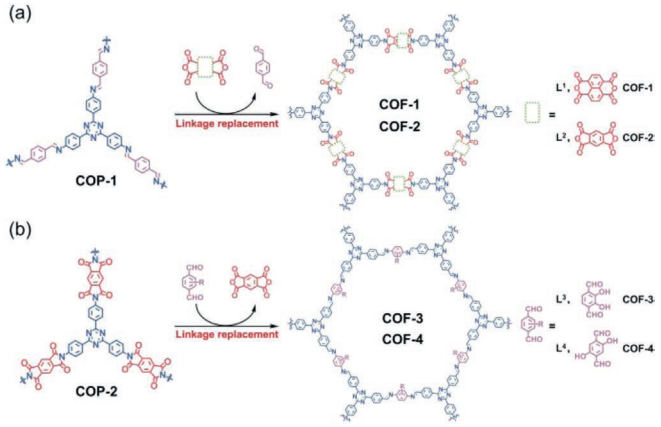


Fig. 7. Conversion of amorphous COPs into COFs using the linkage replacement strategy. Reproduced with permission [63]. Copyright 2019, Wiley-VCH.

2.2.5. Linkage exchange strategy

This strategy is based on ligand exchange [59], which involves the *in situ* replacement of linkers in prepared COFs, transforming them into other COFs with a different structure. Zhao, Horike and Yaghi *et al.* have reported pioneering works in COFs-to-COFs transformation strategy by building block exchange [60–62]. This approach has recently been extended to the conversion between different COFs, and even to the transformation between covalent organic polymers (COPs) and COFs with different bonding architectures. In the process, the original framework can serve as a template to guide the growth of new framework. This approach represents a new direction in COFs chemistry, where the establishment of new linkages is no longer constrained by trial-and-error methods or the inherent uncertainties associated with bottom-up synthesis.

Considering the PI bonds are less reversible than COPs based on dynamic covalent bonds, Zeng *et al.* reported an easy preparation approach of PI-COFs from amorphous COPs through the linkage replacement under different reactions (Fig. 7) [63]. They first synthesized imine-linked COP-1 and amide-linked COP-2, and extended the ligand exchange strategy by introducing an anhydride to convert the imine-linkage COP-1 into amide-linked COF-1 and COF-2, and an aromatic aldehyde to convert the amide-linked COP-2 into imine-linked COF-3 and COF-4, respectively. The COFs with high crystallinity and porosity were fabricated successfully. Then, Lostch *et al.* synthesized Py-imide-COF from the precursor PyTTA with a ligand exchange approach. Firstly, the precursor PyTTA was reacted with PD to synthesize Py1P-COF, and then substituted with PMDA to obtain a high crystallinity and porous Py-imide-COF [41]. The results showed that both the precursor Py1P-COFs and the resulting Py-amide COFs exhibited high crystallinity and the same diffraction patterns, as well as the remained framework after transformation. In addition, the same method has also been utilized to synthesize the redox-active pyrene-containing PI-COFs with high crystallinity through imine-linked COFs as the template [64].

To date, several synthetic methods have been developed for constructing PI-COFs. With increasing insight into the intricate mechanism of the polyimide reaction and its crystallization process [65], it is believed that the preparation of PI-COFs materials with high crystallinity may become easier in the future.

3. Applications of PI-COFs

For PI-COFs, the rich carbonyl groups and N, O heteroatoms in the imide units are both active sites, hopefully for the potential utilization in many applications. Additionally, the periodic porous structure provides ample exposure to active sites and con-

venient channels for mass migration. Furthermore, the high designability in their molecular structures provides high flexibility in the regulation of functionalities and redox abilities. These properties offer great potential for the applications of PI-COFs in adsorption/separation, catalysis, chemical sensing, energy storage and so on. The following sections will introduce some important applications to underscore the vital role of PI linkage in PI-COFs.

3.1. Adsorption/separation

Periodic porous structures and pore size are critical indicators of the adsorption and separation capabilities of PI-COFs. To date, the reported adsorption/separation applications of PI-COFs can be mainly classified as dye adsorption and gas adsorption/separation [11,66]. Yan's group was the first to report the use of 2D PI-COFs for dye separation [11]. Using PMDA as the linker and triamines of different lengths (TAPA, TAPB or TABPB) as a node, they prepared PI-COFs-1, PI-COFs-2 and PI-COFs-3, respectively. As the size of the triamine units increases, PI-COF-3 had the largest pore size (42×53 Å^2). Considering rhodamine B (RB, 10×16 Å^2) had a comparable size to PI-COF-3, RB could be adsorbed by PI-COF-3 by immersing PI-COF-3 in 1.0×10^{-3} mol/L RB for 24 h, which was proved by the decreased S_{BET}. Specifically, the RB-doped PI-COFs showed a strong temperature-dependent fluorescence intensity.

In addition to dye adsorption, PI-COFs can also be applied in gas separation, such as acetylene/ethylene mixture, N_2/O_2 mixture. For instance, at 1 bar and 298 K, the acetylene adsorption of PAF-110 reached 2.23 mmol/g [31], which was almost twice that of ethylene (1.29 mmol/g). It can be seen that PAF has a higher affinity to acetylene (Q_{st}, −38.4 kJ/mol for acetylene and −22.6 kJ/mol for ethylene). Computational simulations indicated there was an enhanced electrostatic interaction between acetylene and the carbonyl oxygen atoms of PAF-110. Except for this, Xue's group studied mixed matrix membranes comprising PI-COFs for N_2/O_2 separation [66]. Unexpectedly, the permeability of N_2 was greater than that of O_2, although the diameter of O_2 (3.46 Å) was smaller than that of N_2 (3.64 Å), which might be due to structural similarities between the N_2 molecule and the melamine unit.

3.2. Catalysis

Since PI-COFs exhibit ultra-strong stability (*e.g.*, acid, alkali, humidity and heat resistance), they can serve as ideal catalytic platforms for catalysis. Moreover, the microenvironment in the cavity of the heteroatom-rich PI-COFs can also generate complicated influences on the active sites and catalytic performances. In addition, the highly in-plane conjugated structures in COFs can facilitate charge transfer. These properties make PI-COFs exhibit great potential for broadening applications in photocatalysis, electrocatalysis or chemical catalysis, *etc*.

3.2.1. Photocatalysis

PI-COFs could exhibit a wide-spectrum absorption, particularly in the visible light range, which makes them ideal candidates for photocatalysis. Recently, some pioneering works on the application of PI-COFs for heterogeneous photocatalysis in organic synthesis have been reported. Zou's group reported a synergy of PI-COFs (*i.e.*, PI-COF-TT) with Ni single sites for selective photocatalysis CO_2 to CO [67]. The excellent selectivity of triazine PI-COFs was mainly due to the functional synergy of PI-COFs that could not only act as photosensitizers to generate photo-generated carriers, but also as carriers to coordinate molecular Ni catalytic site, which was the active site for CO_2 activation and transformation. This work showed that the photoelectrons in PI-COFs were effectively separated from the ring to the diimide bond and then transmitted to the isolated Ni active site, thus driving CO_2 reduction. Not only that, Jiang *et al.* also reported 2D phthalocyanine-based PI-COFs for infrared photomediated phenylsulfide oxidation [43], which unveils the good potential of PI-COFs as photocatalysts. Besides, Kim *et al.* developed a bipyridine-containing PI-COF (PIC-BPY) as a dual redox-active photocatalyst for efficient H_2O_2 generation and pollutant degradation under visible light [68]. Additionally, Zhu *et al.* demonstrated that tuning the electron density of carbonyl groups in PI-COFs could significantly enhance their H_2O_2 photosynthesis performance by modulating the OOH binding energy and internal electric field [69]. Moreover, Xiang *et al.* introduced a strategy for converting imine-linked COFs into benzoxazole-linked COFs *via* post-synthetic oxidation and cyclization, showing improved photocatalytic activity in organic transformations [70]. At present, research on photocatalysis is still rare, and the design of more ligands containing ample photosensitizers and catalytic sites for the application of PI-COF in photocatalysis still needs further exploration.

3.2.2. Electrocatalysis

Electrocatalysis provides an effective method for energy storage and conversion, and is an important way to achieve green and clean energy utilization in the future [71,72]. Jiang *et al.* first assembled 2D phthalocyanine-based PI-COFs (*i.e.*, CoPc-PI-COF-1 and 2) by assembling CoTAPc with PD and BD monomers, respectively (Fig. 8a) [73]. In electrocatalytic CO_2RR, due to both having the same Co(II)-N_4 active sites in PI-COFs, these two CoPc-PI-COFs based cathodes displayed a high and similar faradaic efficiency (FE_{CO}) of 87%–97% (potentials at −0.60 ∼ −0.90 V *vs.* RHE) in 0.5 mol/L $KHCO_3$ solution, similar to the isolate CoPc (Fig. 8d). For the CoPc-PI-COF-1 with shorter linker, its electrode exhibited a higher current density (j_{CO}) than that of CoPc-PI-COF-2 based electrode, which was associated with higher electronic conductivity (Fig. 8e), probably due to longer linker diminishing the conductivity. Interestingly, CoPc-PI-COF-1 also had long-term durability; the TON at −0.70 V (*vs.* RHE) was accumulated to 277,000 for 40 h. Chen *et al.* systematically demonstrated that MPc-PI-COFs have the capability for oxygen reduction (ORR) and oxygen evolution (OER), because the M-N_4 sites with different metals could adjust the binding energy of O-containing intermediates to influence the catalytic activity [49].

The number of electrocatalytic active centers is an essential factor in improving the efficiency of electrocatalysis, and more active electrocatalytic sites will bring higher electrocatalytic performance. Following the first report of COFs with pts topology by Wang *et al.* [74], Jiang *et al.* further constructed the 3D PI-COF (CoPc-PI-COF-3) with interpenetrated *pts* networks (Fig. 8b) [51]. Because the 3D pore structure accounted for 32.7% of the total CoTAPc subunit active site, a higher current density (j_{CO}) of −31.7 mA/cm^2 at −0.90 V and the faradaic efficiency (FE_{CO}) of 88%–96% for the CO_2-to-CO conversion were obtained (Fig. 8f), which were higher than the described above excellent 2D COF analog (Fig. 8g). Besides regulating the pore size, enhancing conjugation degrees is another way to improve the electrocatalytic performance [75]. Introducing electron-donating conjugation units into COFs is beneficial for the electrocatalytic process. Peng *et al.* fabricated two phthalocyanine-porphyrin-based PI-COFs (*i.e.*, CoPc-2H_2PP and CoPc-H_2PP) using CoPc as nodes to couple with DAPP or TAPP as the linker, respectively (Fig. 8c) [45]. The introduction of electron-rich porphyrin building blocks was beneficial for modulating charge transfer ability and regulating the conjugation structure. Despite possessing a less active catalytic site, CoPc-2H_2PP still exhibited higher current density, FE_{CO}, and CO selectivity with a lower overpotential than CoPc-H_2PP. The entire mechanistic pathway involved the activation of active Co(II) site, the adsorption and activation of CO_2, the formation and conversion of *COOH intermediate, as well as the formation and desorption of *CO resulting in CO (Figs. 8h and i). Among these steps, the formation of *COOH intermediate was the

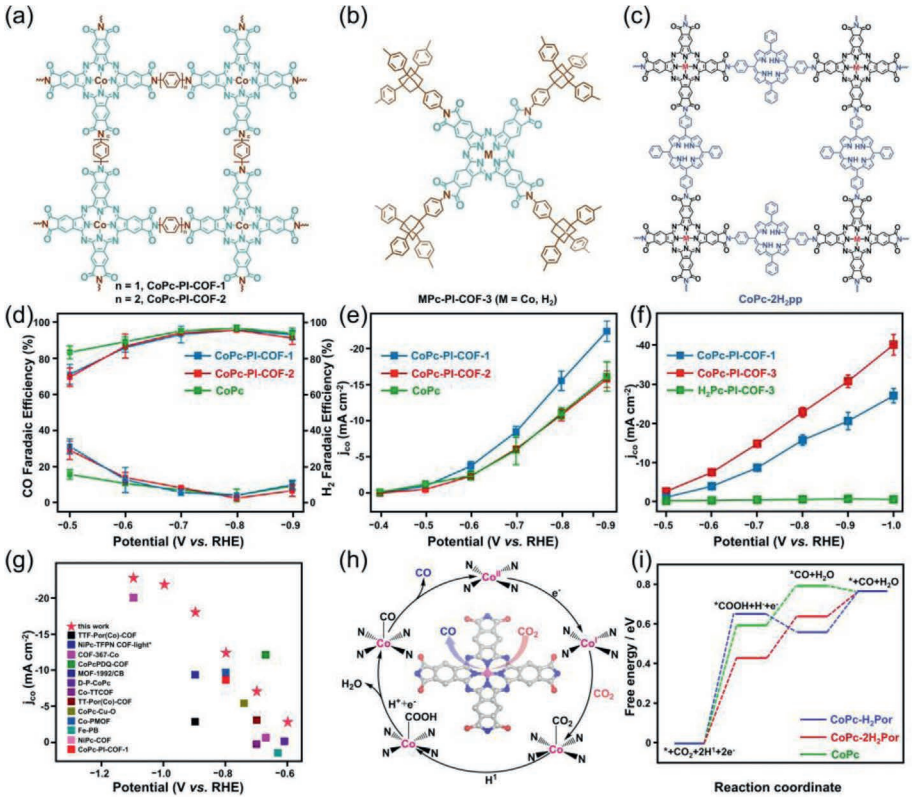


Fig. 8. Schematic representation and electrocatalytic CO_2RR performances of the four phthalocyanine-based PI-COFs. (a) 2D CoPc-PI-COF, Reproduced with permission [73]. Copyright 2021, American Chemical Society. (b) 3D CoPc-PI-COF-3. Reproduced with permission [51]. Copyright 2021, Wiley-VCH. (c) CoPc-2H_2Por. Reproduced with permission [45]. Copyright 2022, Wiley-VCH. (d) Faradaic efficiency. (e) Partial CO current density. Reproduced with permission [73]. Copyright 2021, American Chemical Society. (f) Faradaic efficiency. (g) j_{CO} of CoPc-PI-COF-3 in H-type electrochemical cell. Reproduced with permission [51]. Copyright 2021, Wiley-VCH. (h) Proposed mechanism and (i) free energy diagram for the CO_2RR process of CoPc-2H_2Por. Reproduced with permission [45]. Copyright 2022, Wiley-VCH.

crucial rate-determining step. The Gibbs free energy of *COOH at CoPc-2H_2PP was the lowest compared to CoPc-H_2PP and the isolated CoPc. Recently, Lan *et al.* also employed this strategy for efficient electrocatalytic CO_2 reduction coupled with methanol oxidation [19]. Larger pore structure and higher conjugation not only facilitated the enrichment, adsorption, and electron transfer of CO_2, but also reduced the activation energy barrier of the reaction, thereby enhancing the electrocatalytic performance.

The conductivity is also an important influential factor in electrocatalytic reactions. Enhancing electrical conductivity can effectively regulate the electronic transport capacity of materials. Recently, 2D phthalocyanine PI-COFs (NiPc-OH–COF) have been designed between NiPc and 2,5-diamino-1,4-benzenediol (DBO) [44]. NiPc-OH–COF exhibited conductivity that could be as high as 1.5×10^{-3} S/m, which was due to the introduction of −OH and the formation of strong hydrogen bonds in the O–H of DBO in adjacent layers. It exhibited an almost 100 % CO_2-to-CO faradaic efficiency and a high TOF value.

Electrocatalysis is a complicated reaction process, where typically no single factor plays a decisive role. Combining various factors such as chemical composition, topology structure, specific surface area and crystallinity, they together determine the final electrocatalytic performance. These works listed above provide a good start for PI-COFs as the key electrocatalysts, and more PI-COFs electrocatalysts with high efficiency and selectivity are being developed.

3.2.3. Chemical catalysis

In addition to photo-/elecro-electrocatalysis, PI-COFs can also be employed in traditional chemical catalysis. To date, only a few studies have been reported, primarily focusing on anchoring metals onto PI-COFs for catalytic reactions. Typically, metal sites can be effectively loaded onto the imide functional groups in the PI-COFs frameworks through covalent bonding, ensuring the uniform distribution of metal sites. Alternatively, the reducing atmosphere can be used to reduce metal ions into metal nanoparticles, which are then incorporated into the PI-COFs frameworks, resulting in highly active metal nanoparticle sites. These metal sites not only provide additional catalytic activity but also enhance electron transfer efficiency through the synergistic interaction between metal nanoparticles and PI-COFs, thereby improving the selectivity and activity. For example, Pd@PI-COFs were used in the Suzuki–Miyaura coupling reaction [76]. Moreover, other examples like Cu(II)/PI-COFs also served as the catalysts for the synthesis of 2,4,5-trisubstituted imidazole using the solvent-free microwave irradiation [77], and the Chan-Lam coupling reaction [78].

3.3. Chemical sensing

Xian's group successfully synthesized fluorescent PI-COFs using TAPP and PTCA for the detection of 2,4,6-trinitrophenol (TNP) [14]. This may be ascribed to the integration of electron transfer between PI-CONs and TNP and the inner filter effect based on spectral overlap data and DFT calculations. Yang *et al.* synthesized two new PI-COFs (*i.e.*, PI-COF-201 and PI-COF-202), in which PI-COF-201 exhibited high fluorescence selectivity toward Fe^{3+} [46]. The high performance was ascribed to the efficient energy transfer from the emission state of PI-COF-201 to the unoccupied d-orbital of Fe^{3+}, leading to the quenching of PI-COF-201 fluorescence. Besides, Hu *et al.* developed a smart photo-assisted fluorescent PI-COF-based sensor capable of visually detecting Pb^{2+} with high sensitivity and a detection limit as low as 100 pmol/L under UV light,

demonstrating great potential for on-site heavy metal monitoring [79]. Not only that, PI-COFs also showed excellent sensing performance in detecting antibiotics [80], especially for the measurement of the known concentration of tetracycline and ofloxacin, the detection efficiency reached up to 98 %–110 %.

3.4. Energy storage

With the rapid development of renewable energy, energy storage has become increasingly crucial in modern energy systems [81]. PI-COFs have emerged as one of the promising materials for energy storage applications due to their O- and N-rich nature, which facilitates effective cationic charge stabilization. As the metal ion battery electrode material, PI-COFs have the following advantages: (1) Abundant redox active sites for charge storage; (2) The unique π-π conjugated structure can reduce the energy level of intermolecular charge transfer, which is more conducive to ion transport and electron conduction; (3) PI-COFs have good structural designability and can be adjusted and optimized by selecting different organic groups and coordination metal ions. So far, PI-COFs have been applied in lithium-ion batteries, Zn-ion batteries, sodium-ion batteries, and so on.

3.4.1. Lithium-ion batteries (LIBs)

LIBs have been widely used in daily electronic devices, and more and more organic electrode materials are needed because of their advantages such as large capacity, designable molecular structure and environmental friendliness [82]. Considering that many organic electrode materials might generate radical intermediates during multiple redox processes, charge-discharge capacity and rate as well as cycle stability are important factors in the design of electrode materials [83,84]. Not only that, several other factors are also critical, such as the high-density active sites, low solubility and fast kinetic response. PI-COFs combine the advantages of both PI and COFs, providing an excellent solution to the above problems.

Sun *et al.* developed an atomic-layer PI-COFs (*i.e.*, E-TP-COF) with a dual-active center of C=O and C=N group that can be applied as cathode materials in LIBs [32]. Using the atomic-layer-thick structure and triazine core to improve the capture and diffusion of Li^+. The Li^+ batteries assembled with E-TP-COF deliver a high original capacity of 110 mAh/g with 87.3 % capacity retention after 500 cycles. Both active sites of C=N and C=O groups could generate more capacity [85,86]. To further increase the theoretical capacity of battery, the most efficient approach is to increase the density of active sites [87]. Therefore, Jiang *et al.* fabricated mesoporous PI-COFs (HATN-AQ-COF) as the cathodes for LIBs [17]. The introduction of more N atoms in the core HATN can not only enhance the affinity of Li^+, but also improve the number of active sites (Fig. 9a). Moreover, the monomer DAAQ is also considered as the active site of Li^+ storage. With more active sites (C=N, C=O), HATN-AQ-COF achieved a high reversible capacity of 319 mAh/g at 0.5 C (theoretical capacity, 358 mAh/g). The theoretical number of Li^+ stored per asymmetric unit of HATN-AQ-COF was 12, in which 6 Li^+ located in the HATN moieties (site A), 3 Li^+ located in the quinone groups (site B), and 3 Li^+ located in the imide moieties (site C), which was divided into four successive $3e^-$ steps (Fig. 9b). Coincidentally, Chen *et al.* selected CoTAPc-based PI-COFs by reacting the anhydride CoTAPc with three linker lengths of phenediamine monomer (PDA, BDA and TDA) [88]. The C=O in anhydride and C=C/C=N in phthalocyanine macrocyclic all could combine with Li^+, which followed a two-step lithium-embedding process, and one CoTAPc-based PI-COFs could embed up to 52 Li^+.

To further increase the density of active sites, apart from the N atom, the introduction of more carbonyl groups has also been

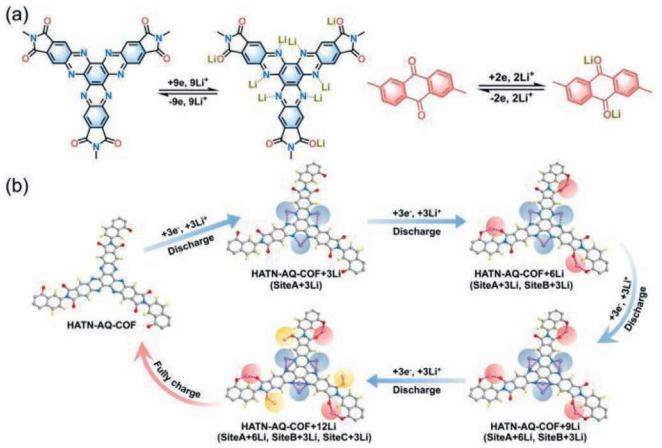


Fig. 9. Possible lithium storage processes of HATN-AQ-COF. (a) The lithium binding sites of HATN-AQ-COF. (b) Possible lithium storage process of HATN-AQ-COF. Reproduced with permission [17]. Copyright 2022, Wiley-VCH.

shown to be effective. Liu and Fang *et al.* introduced two 2D PI-COFs (*i.e.*, COF-JLU85 and COF-JLU86), synthesized by combining TRO with PMDA and NTCDA, respectively [42]. These PI-COFs possessed a unique 18-carbonyl redox-active site per pore and were evenly distributed along the pore walls. With high-density carbonyl redox-active sites, the optimal COF-JLU86 delivered excellent anode performance with an extremely high specific capacity of 1161.1 mAh/g at 0.1 A/g, and impressive cycling stability retaining 401.1 mAh/g at 15 A/g after 10,000 cycles, higher than that previously reported organic polymer materials. Regulating high crystallinity is another way to improve battery performance. Wang *et al.* developed a PI-$COF_{TPDA\text{-}PMDA}$ constitude of TPDA and PMDA ligands [40]. By virtue of high crystallinity and dual-active center, PI-$COF_{TPDA\text{–}PMDA}$ as a cathode material, delivered a high initial charge capacity of 233 mAh/g (0.5 A/g) and cycling stability. In addition, PI-COFs can also be employed in lithium-sulfur batteries (LSBs) [16,89–91], which can physically or chemically confine soluble LiPSs into well-defined porous structures of PI-COFs to conquer the possible challenges of LSBs to some extent.

3.4.2. Zn-ion batteries (ZIBs)

Rechargeable ZIBs, a kind of safe and economical energy storage technique, have shown great potential as next-generation battery systems [92]. Combined the possible zincophilic sites (*e.g.*, C=O and C–N) with the ordered pore structure, PI-COFs show great advantages in Zn^{2+} batteries. For instance, Feng *et al.* fabricated an organic Zn^{2+}-storage anode constructed by 2D NTCDA-based PI-COFs [50]. The well-defined pore channels of PI-COFs make the internal carbonyl active site have higher accessibility to Zn^{2+} and a lower energy barrier for ion diffusion at a low potential window. Therefore, this PI-COF-based anode showed a high specific capacity (332 C/g at 0.7 A/g) and long-cycle ability. Yan *et al.* also designed aqueous ZIBs based on NTCDA-based PI-COFs [93], which delivered an ultrahigh C=O or C=N along with the pore channels. To further understand the mechanism of Zn^{2+} storage, Lan *et al.* proposed a unique zigzag hopping mechanism by constructing anhydride-based PI-COFs [94]. They pointed out that ABC stacked anhydride PI-COFs with specific sites can simultaneously promote Zn^{2+} migration, shorten diffusion path, reduce diffusion energy barrier, and accelerate Zn^{2+} diffusion kinetics, thus exhibiting uniform ion flux, low nucleation overpotential and good hydrogen evolution inhibition to obtain excellent electrochemical properties.

3.4.3. Sodium-ion batteries (SIBs)

SIBs and LIBs have the same working principle, so it is expected to replace commercial LIBs to reduce the risk of lithium source

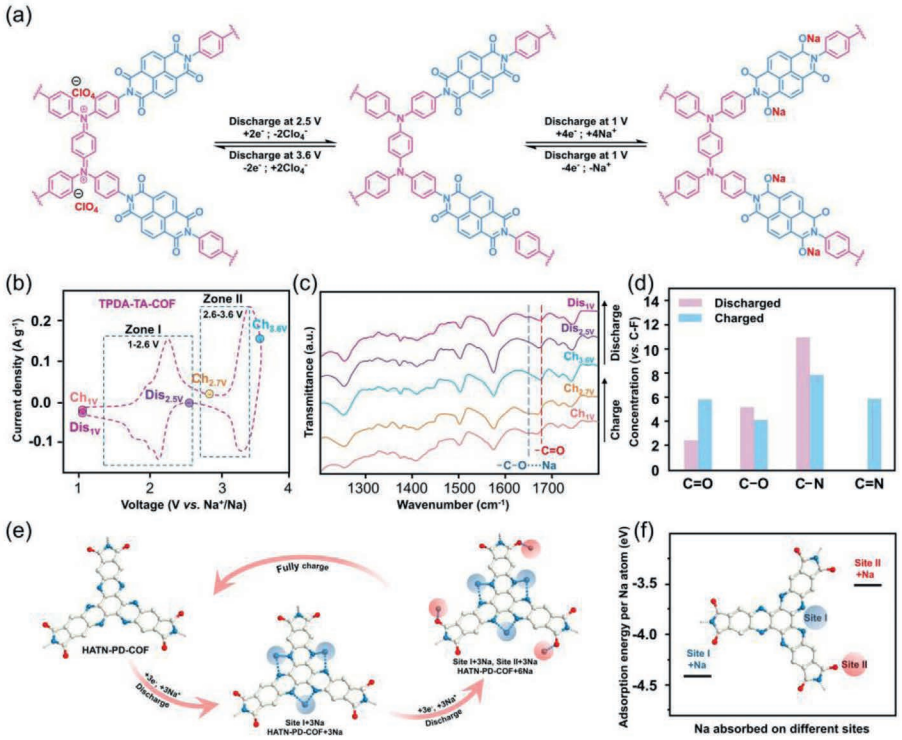


Fig. 10. Redox mechanism and characterization during the charging-discharging process of TPDA-NDI-COF and HATN-PD-COF. (a) Mechanism investigation of TPDA-NDI-COF in $NaClO_4$. (b) CV of charge and discharge profile and (c) *ex-situ* FT-IR spectra. (d) The concentration of bond intensities during the charging and discharging process. Reproduced with permission [101]. Copyright 2024, Wiley-VCH. (e) Structural evolution during the sodiation/desodiation process. (f) The adsorption energy per Na^+ ion of HATN-PD-COF. Reproduced with permission [20]. Copyright 2024, Springer Nature.

shortages and price fluctuations [95]. However, since the radius of Na^+ (0.102 nm) is larger than that of Li^+ (0.076 nm), the molar mass of sodium is much greater than that of lithium, and the capacity of SIBs is often inferior to that of LIBs [96,97]. At present, the lack of suitable sodium storage materials has greatly limited the development of SIBs, and the development of high-capacity and long-life electrode materials is crucial to achieving the large-scale application of SIBs.

PI-COFs possess porous channels that facilitate the rapid shuttle of ions in the charge and discharge process, weaken the volume expansion of electrode materials, and improve the rate performance of batteries [98,99]. At the same time, the highly adjustable structures allow the skeletons can be embedded in a rich discharge site, and the theoretical specific capacity of the battery can be improved [100]. For example, a p/n-type TPDA-NDI-COF, as the cathode material, was constructed for SIBs by TPDA and NDA with the solvothermal method [101]. The prepared TPDA-NDI-COF showed a wide potential window (1.0–3.6 V *vs.* Na^+/Na) with a double redox active center and provided a specific capacity of 67 mAh/g at 0.05 A/g. TPDA-NDI-50 % CNTs exhibited strong cycling stability, maintaining a battery capacity of 92 mAh/g even after 10,000 cycles at 1.0 A/g. This indicates that the C−N bond is responsible for the reaction of the electrolyte anion in the high potential region II, and the C=O bond tends in the low potential region I to react with Na^+ (Figs. 10a-d). In addition, Jiang *et al.* also synthesized HATN-PD-COF and HATN-TAB-COF with redox-active monomer (*i.e.*, HAT-NCA) as the cathode materials of SIBs [20]. Due to the existence of abundant active C=N/C=O groups, and high stability, the prepared PI-COFs cathodes presented high reversible capacities with a record-high rate, and long-term stability (the capacity retention was nearly 91 % at 10,000 mA/g after 7000 cycles). The calculated results and adsorption energies diagram demonstrated that HATN-PD-COF followed a two-step $3e^-$ sodiated procedure during the sodiation/desodiation process, *i.e.*, HATN-PD-COF+3Na (site I + 3Na) and HATN-PD-COF + 6Na (site II + 3Na). The efficient Na^+ diffusion with a low diffusion energy barrier along the mesoporous tunnel showed ultrafast and stable Na^+ storage (Figs. 10e and f). In addition, structural regulation after synthetic vulcanization has also been used for enhancing the performance of cathodes in PI-COFs [46]. Lu *et al.* prepared the 2D PI-COFs (TAPA-COFs) with NTCDA and TAPA or TT monomers, respectively. Due to the higher activity of C=S to Na^+, the Lawesson reagent was selected to realize the conversion of C=O bond in TAPA-COFs to C=S bond, resulting in the enhanced surface activity of TAPA-COFs. The above works show the potential of PI-COFs in improving the performance of SIBs, which might advance the development of new porous materials for energy storage.

In addition, PI-COFs have also shown great interest in aluminum-ion batteries [33], potassium-ion batteries [102], Mn-ion batteries [103], proton batteries [104], *etc.* Although PI-COFs have many advantages in energy storage, there are still some problems that cannot be ignored: (1) The LUMO of the π-π conjugated system in most PI-COFs has a high energy level, which makes the redox potential low; (2) There are insufficient redox active sites available in PI-COFs nanochannels, which is not conducive to efficient metal ions transport; (3) Highly active lithium metal is easy to react with the liquid electrolyte, forming an unstable solid electrolyte phase, causing uneven lithium deposition to result in low coulomb efficiency (CE) and rapid capacity decay [105]. To improve the applicability of PI-COFs in energy storage, it is necessary to expand the perspective from molecular design to structural design and in-depth understanding of the mechanism in the subsequent research.

4. Perspective

Since the first report in 2014, PI-COFs have developed rapidly in various fields. Compared to PI polymers and other COFs, PI-COFs offer several notable advantages, (1) the imide ring structure, as well as the conjugated interactions and hydrogen bond-

ing between the densely packed conjugated aromatic framework of PI-COFs confer excellent thermal stability and high chemical inertness; (2) with highly controllable porous structure and functional groups containing heteroatoms, PI-COFs can provide abundant active sites for reversible deintercalation of metal ions in cathode materials, which is conducive to increasing energy density and accelerating electrochemical reaction rate and (3) by designing monomers or utilizing synthetic methods, PI-COFs with varied functional groups and tunable porosity can be tailored for diverse applications.

Looking forward to the future, the research of PI-COFs is still in its infancy. (1) There is great demand for designing and synthesizing more monomers and building blocks of functional PI-COFs. Given the low reversibility of the imidization reaction, the synthesis method still needs strict reaction conditions and environments, and high crystallinity and large-scale syntheses of PI-COFs are still challenging. Structural engineering, function tuning, and mechanistic study of synthesis process may offer some promising strategies to overcome these synthetic challenges. (2) Although PI-COFs have abundant redox active sites, the tight π-π stacking between the interlayers makes most of the active groups unable to be effectively exposed, resulting in low mass transport efficiency. Strategies like designing mesopores, creating defects, adding multi-functions or controlling morphology would be of great significance for improving the comprehensive properties of PI-COFs. (3) Whether it is catalysis, battery, or sensing applications, they all involve energy transfer and storage, including adsorption/desorption, exciton separation and energy transfer processes, *etc*., which need overall design to synergistically tune their functions. Some advanced techniques like machine learning or artificial intelligence can be combined to guide the specific design of PI-COFs for target properties. Meanwhile, potential interdisciplinary applications, especially in biomedicine or environmental engineering, in addition to currently developed application fields, may open new opportunities and expand the scope of PI-COFs.

5. Summary

In this review, we have comprehensively summarized the recent progress toward PI-COFs, including the design characteristics, synthesis, related applications and mechanism as well as the structure-to-property relationship. We also navigate and discuss their challenge and opportunities in the future from the perspectives of material or chemical science. We hope that this review could provide readers with a comprehensive understanding of the fundamental characteristics, modulation strategies, key applications, current challenges, and future developments of PI-COFs, thereby stimulating broader research interest in this field.

Declaration of competing interest

The authors declare that they have no known competing financial interests or personal relationships that could have appeared to influence the work reported in this paper.

CRediT authorship contribution statement

Qi Li: Writing – review & editing, Writing – original draft, Investigation, Conceptualization. **Minqiao Liang:** Writing – original draft, Investigation. **Huifen Zhuang:** Software, Methodology. **Zhengyang Chen:** Investigation. **Yuxiang Jiang:** Investigation. **Xiaofei Chen:** Writing – review & editing, Writing – original draft, Funding acquisition, Conceptualization. **Yifa Chen:** Writing – review & editing, Funding acquisition, Conceptualization. **Ya-Qian Lan:** Writing – review & editing, Funding acquisition, Conceptualization.

Acknowledgments

This work was financially supported by the National Key R&D Program of China (No. 2023YFA1507204). National Natural Science Foundation of China (Nos. 22475074, 22171139, 22225109, 22302055). Natural Science Foundation of Guangdong Province (No. 2023B1515020076). Key Scientific Research Project Plan of Colleges and Universities of Henan Province (No. 24B150004). The Double Thousand Talents Plan of Jiangxi Province (No. jxsq2023102003). Project supported by the Guangdong Provincial Key Laboratory of Carbon Dioxide Resource Utilization (No. 2024B121201001). Project supported by the Major Research plan of the National Natural Science Foundation of China (No. 92461310).

References

[1] M.T. Bogert, R.R. Renshaw, J. Am. Chem. Soc. 30 (1908) 1135–1144.
[2] F.M. Toma, F. Puntoriero, T.V. Pho, et al., Angew. Chem. Int. Ed. 54 (2015) 6775–6779.
[3] V.L. Bell, B.L. Stump, H. Gager, J. Polym. Sci. Pol. Chem. 14 (1976) 2275–2291.
[4] I. Gouzman, E. Grossman, R. Verker, et al., Adv. Mater. 31 (2019) 1807738.
[5] X.J. Liu, M.S. Zheng, G. Chen, et al., Energy Environ. Sci. 15 (2022) 56–81.
[6] Y. Wang, Y. Cui, Z. Shao, et al., Chem. Eng. J. 390 (2020) 124623.
[7] T.B. Schon, A.J. Tilley, E.L. Kynaston, et al., ACS Appl. Mater. Interfaces 9 (2017) 15631–15637.
[8] B.S. Ghanem, N.B. McKeown, P.M. Budd, et al., Adv. Mater. 20 (2008) 2766–2771.
[9] O.K. Farha, A.M. Spokoyny, B.G. Hauser, et al., Chem. Mater. 21 (2009) 3033–3035.
[10] J. Weber, Q. Su, M. Antonietti, et al., Macromol. Rapid Commun. 28 (2007) 1871–1876.
[11] Q. Fang, Z. Zhuang, S. Gu, et al., Nat. Commun. 5 (2014) 4503.
[12] Q. Fang, J. Wang, S. Gu, et al., J. Am. Chem. Soc. 137 (2015) 8352–8355.
[13] D. Yang, Z. Yao, D. Wu, et al., J. Mater. Chem. A 4 (2016) 18621–18627.
[14] C. Zhang, S. Zhang, Y. Yan, et al., ACS Appl. Mater. Interfaces 9 (2017) 13415–13421.
[15] B. Sun, X. Li, T. Feng, et al., ACS Appl. Mater. Interfaces 12 (2020) 51837–51845.
[16] H. Duan, K. Li, M. Xie, et al., J. Am. Chem. Soc. 143 (2021) 19446–19453.
[17] X. Yang, L. Gong, X. Liu, et al., Angew. Chem. Int. Ed. 61 (2022) e202207043.
[18] T. Kim, S.H. Joo, J. Gong, et al., Angew. Chem. Int. Ed. 61 (2022) e202113780.
[19] M. Zhang, J.P. Liao, R.H. Li, et al., Nat. Sci. Rev. 10 (2023) nwad226.
[20] X. Yang, L. Gong, Z. Liu, et al., Sci. China Chem. 67 (2024) 1300–1310.
[21] A.P. Côté, A.I. Benin, N.W. Ockwig, et al., Science 310 (2005) 1166–1170.
[22] Y. Yang, Q. Li, P. Liu, et al., Adv. Mater. 37 (2025) 2415799.
[23] H. Dong, L. Fang, K.-X. Chen, et al., Angew. Chem. Int. Ed. 64 (2025) e202414287.
[24] J. Lv, Y.X. Tan, J. Xie, et al., Angew. Chem. Int. Ed. 57 (2018) 12716–12720.
[25] R. Xu, D.H. Si, S.S. Zhao, et al., J. Am. Chem. Soc. 145 (2023) 8261–8270.
[26] W. Feng, C. Guo, R. Xu, et al., Coord. Chem. Rev. 515 (2024) 215965.
[27] K.V. Rao, R. Haldar, C. Kulkarni, et al., Chem. Mater. 24 (2012) 969–971.
[28] K.V. Rao, R. Haldar, T.K. Maji, et al., Polymer 55 (2014) 1452–1458.
[29] Y. Zhang, Z. Huang, B. Ruan, et al., Macromol. Rapid Commun. 41 (2020) 2000402.
[30] B. Yao, G. Li, X. Wu, et al., Chem. Comm. 60 (2024) 793–803.
[31] L. Jiang, Y. Tian, T. Sun, et al., J. Am. Chem. Soc. 140 (2018) 15724–15730.
[32] G. Zhao, H. Li, Z. Gao, et al., Adv. Funct. Mater. 31 (2021) 2101019.
[33] Y. Liu, Y. Lu, A.H. Khan, et al., Angew. Chem. Int. Ed. 62 (2023) e202306091.
[34] R. Van der Jagt, A. Vasileiadis, H. Veldhuizen, et al., Chem. Mater. 33 (2021) 818–833.
[35] Y. Luo, Z. Chang, J. Pei, et al., Nano Lett. 23 (2023) 9266–9271.
[36] S.K. Upadhyay, S.R.K. Pingali, B.S. Jursic, Tetrahedron Lett. 51 (2010) 2215–2217.
[37] L. Kurti, B. Czako, Strategic Applications of Named Reactions in Organic Synthesis, Elsevier Academic Press, Burlington, MA, 2005, pp. 202–203.
[38] K. Geng, T. He, R. Liu, et al., Chem. Rev. 120 (2020) 8814–8933.
[39] J. Maschita, T. Banerjee, G. Savasci, et al., Angew. Chem. Int. Ed. 59 (2020) 15750–15758.
[40] L. Yao, C. Ma, L. Sun, et al., J. Am. Chem. Soc. 144 (2022) 23534–23542.
[41] J. Maschita, T. Banerjee, B.V. Lotsch, Chem. Mater. 34 (2022) 2249–2258.
[42] J. Li, J. Zhang, Y. Hou, et al., Angew. Chem. Int. Ed. 63 (2024) e202412452.
[43] X. Zhan, Y. Jin, B. Han, et al., Chin. J. Catal. 69 (2025) 271–281.
[44] M. Li, B. Han, S. Li, et al., Small 20 (2024) 2310147.
[45] J. Yuan, S. Chen, Y. Zhang, et al., Adv. Mater. 34 (2022) 2203139.
[46] T. Wang, R. Xue, H. Chen, et al., New J. Chem. 41 (2017) 14272–14278.
[47] K. Liu, H. Qi, R. Dong, et al., Nat. Chem. 11 (2019) 994–1000.
[48] J. Shi, W. Tang, B. Xiong, et al., Chem. Eng. J. 453 (2023) 139607.
[49] Y. Li, J. Tan, X. Zhao, et al., Mater. Today Commun. 37 (2023) 107157.
[50] M. Yu, N. Chandrasekhar, R.K.M. Raghupathy, et al., J. Am. Chem. Soc. 142 (2020) 19570–19578.
[51] B. Han, Y. Jin, B. Chen, et al., Angew. Chem. Int. Ed. 61 (2022) e202114244.
[52] S. Kandambeth, K. Dey, R. Banerjee, J. Am. Chem. Soc. 141 (2019) 1807–1822.

[53] R. Liu, K.T. Tan, Y. Gong, et al., Chem. Soc. Rev. 50 (2021) 120–242.
[54] H. Zhuang, C. Guo, J. Huang, et al., Angew. Chem. Int. Ed. 63 (2024) e202404941.
[55] C.S. Diercks, O.M. Yaghi, Science 355 (2017) eaal1585.
[56] O. Rahmanian, M. Falsafin, M. Dinari, Polym. Int. 69 (2020) 712–718.
[57] Z. Wang, Y. Zhang, J. Liu, et al., Nat. Protocols 19 (2024) 3489–3519.
[58] T. Kim, B. Park, K.M. Lee, et al., ACS Macro Lett. 7 (2018) 1480–1485.
[59] P. Deria, J.E. Mondloch, O. Karagiaridi, et al., Chem. Soc. Rev. 43 (2014) 5896–5912.
[60] C. Qian, Q.Y. Qi, G.F. Jiang, et al., J. Am. Chem. Soc. 139 (2017) 6736–6743.
[61] G. Zhang, M. Tsujimoto, D. Packwood, et al., J. Am. Chem. Soc. 140 (2018) 2602–2609.
[62] P.J. Waller, S.J. Lyle, T.M. Osborn Popp, et al., J. Am. Chem. Soc. 138 (2016) 15519–15522.
[63] Y. Zhai, G. Liu, F. Jin, et al., Angew. Chem. Int. Ed. 58 (2019) 17679–17683.
[64] M.K. Shehab, K.S. Weeraratne, O.M. El-Kadri, et al., Macromol. Rapid Commun. 44 (2023) 2200782.
[65] V.A. Kuehl, M.J. Wenzel, B.A. Parkinson, et al., J. Mater. Chem. A 9 (2021) 15301–15309.
[66] X. Yuan, Y. Wang, G. Deng, et al., Polym. Adv. Technol. 30 (2019) 417–424.
[67] X. Chen, Q. Dang, R. Sa, et al., Chem. Sci. 11 (2020) 6915–6922.
[68] T. Kim, D.Y. Lee, E. Choi, et al., Appl. Catal. B: Environ. Energy 357 (2024) 124264.
[69] W. Chi, B. Liu, Y. Dong, et al., Appl. Catal. B: Environ. Energy 355 (2024) 124077.
[70] Y. Zhu, D. Huang, W. Wang, et al., Angew. Chem. Int. Ed. 63 (2024) e202319909.
[71] X. Yao, G. Liu, Y. Huang, et al., Angew. Chem. Int. Ed. 64 (2025) e202417439.
[72] Y. Wang, M. Yue, G. Liu, et al., Angew. Chem. Int. Ed. 64 (2025) e202413030.
[73] B. Han, X. Ding, B. Yu, et al., J. Am. Chem. Soc. 143 (2021) 7104–7113.
[74] G. Lin, H. Ding, D. Yuan, et al., J. Am. Chem. Soc. 138 (2016) 3302–3305.
[75] M. Li, B. Han, L. Gong, et al., Chin. Chem. Lett. 37 (2026) 110590.
[76] Z. Dong, H. Pan, P. Gao, et al., Catal. Lett. 152 (2022) 299–306.
[77] M. Sedaghat, F. Moeinpour, F.S. Mohseni-Shahri, Anal. Sci. Adv. 4 (2023) 302–311.
[78] Y. Han, M. Zhang, Y.Q. Zhang, et al., Green Chem. 20 (2018) 4891–4900.
[79] L. Yu, L. Bai, J. Liu, et al., Talanta 295 (2025) 128346.
[80] N. Zhao, J.M. Liu, F.E. Yang, et al., ACS Appl. Bio Mater. 4 (2021) 995–1002.
[81] J. Ma, C. Wang, Q. Liu, et al., Adv. Funct. Mater. 35 (2025) 2419752.
[82] H. Schlomberg, J. Kröger, G. Savasci, et al., Chem. Mater. 31 (2019) 7478–7486.
[83] S. Gu, Y. Chen, R. Hao, et al., Chem. Comm. 57 (2021) 7810–7813.
[84] L. Xu, X. Wang, Y. Wu, et al., J. Energy Chem. 102 (2025) 63–72.
[85] X. Wu, S. Zhang, X. Xu, et al., Angew. Chem. Int. Ed. 63 (2024) e202319355.
[86] Y. Qian, Z. Liu, H. Song, et al., Chin. Chem. Lett. 35 (2024) 108785.
[87] Z. Wang, Y. Li, P. Liu, et al., Nanoscale 11 (2019) 5330–5335.
[88] L. Wang, J. Zhao, J. Chen, et al., Phys. Chem. Chem. Phys. 25 (2023) 8050–8063.
[89] P. Chen, Z. Wu, T. Guo, et al., Adv. Mater. 33 (2021) 2007549.
[90] Z.L. Xu, S. Lin, N. Onofrio, et al., Nat. Commun. 9 (2018) 4164.
[91] X. Xiao, L. Zou, H. Pang, et al., Chem. Soc. Rev. 49 (2020) 301–331.
[92] F. Ji, S. Gou, J. Tang, et al., Chem. Eng. J. 474 (2023) 145786.
[93] Y. An, H. Zhang, D. Geng, et al., Chem. Eng. J. 477 (2023) 147275.
[94] C. Guo, X. Huang, J. Huang, et al., Angew. Chem. Int. Ed. 63 (2024) e202403918.
[95] S.W. Ke, W. Li, L. Gao, et al., Angew. Chem. Int. Ed. 64 (2025) e202417493.
[96] Y. Park, D.S. Shin, S.H. Woo, et al., Adv. Mater. 24 (2012) 3562–3567.
[97] C. Wang, Y. Xu, Y. Fang, et al., J. Am. Chem. Soc. 137 (2015) 3124–3130.
[98] Y. Zang, D.Q. Lu, Y.Q. Lan, Sci. Bull. 67 (2022) 1621–1624.
[99] K. Hua, L. Zhang, Q. Ma, et al., Chem. Eng. J. 498 (2024) 155289.
[100] D. Geng, H. Zhang, Z. Fu, et al., Adv. Sci. 11 (2024) 2407073.
[101] S. Jindal, Z. Tian, A. Mallick, et al., Small 21 (2025) 2407525.
[102] X.X. Luo, W.H. Li, H.J. Liang, et al., Angew. Chem. Int. Ed. 61 (2022) e202117661.
[103] L. Cai, L. Lu, Y. Lan, et al., Adv. Energy Mater. 13 (2023) 2301631.
[104] Y. Yang, S. Wang, Y. Duan, et al., Angew. Chem. Int. Ed. 137 (2025) e202418394.
[105] P.Y. Zhao, Y.H. Zhang, B.Y. Sun, et al., Angew. Chem. Int. Ed. 64 (2024) e202317106.



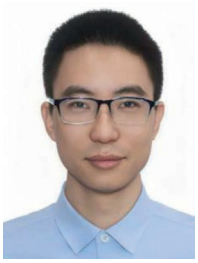
Qi Li received his M.S. degree (2019) from Nanjing Normal University and his Engineering Ph.D. degree (2024) from Southeast University under the supervision of Prof. Zeng-Mei Wang and in collaboration with Prof. Ya-Qian Lan. Since 2024, he has been conducting postdoctoral research at South China Normal University with Prof. Yifa Chen. His current research focuses on the syntheses of COF-based crystalline porous materials and their applications in energy storage and conversion.



Minqiao Liang was born in 2004 in Guangdong, China. She is now a chemistry undergraduate at South China Normal University under the supervision of Prof. Ya-Qian Lan and Prof. Yifa Chen. Her research interest focuses on the syntheses of crystalline porous materials (COF-based composites) and their applications in energy storage and conversion.



Xiaofei Chen received her Ph.D. degree in polymer chemistry and physics from Jilin University under the supervision of Prof. Lixin Wu in 2021. Currently, she works at the Key Laboratory for Special Functional Materials of the Ministry of Education, Henan University, China. Her current research focuses on the syntheses of polyoxometalate based supramolecular complexes as well as COF and their applications in photocatalysis and photothermal catalysis.



Yifa Chen received his B.S. degree from School of Chemistry, Beijing Institute of Technology. He subsequently obtained his Ph.D. degree from School of Chemistry and Chemical Engineering, Beijing Institute of Technology under the supervision of Prof. Bo Wang. In 2022, he joined South China Normal University (SCNU, China) as a professor of chemistry. His research interest focuses on the fabrication of porous crystalline material based devices like membranes, foams and fibers that can be applicable in photo-/electro-catalysis, energy storage or environment treatment.



Ya-Qian Lan received his B.S. and Ph.D. degrees (2009) from Northeast Normal University under the supervision of Prof. Zhong-Min Su. In 2010, he joined the National Institute of Advanced Industrial Science and Technology (AIST, Japan) as a JSPS postdoctoral fellow. In 2012, he became a professor of chemistry at Nanjing Normal University (NNU, China). In 2021, he joined South China Normal University (SCNU, China) as a professor of chemistry. His current research interest focuses on the synthesis of new crystalline materials and catalytic research related to clean energy applications.